

Original Article

Cite this article: Duke K, Ahmad S, and Lau A. (2023) A Monte Carlo study of the dose enhancement effects of high-z foils in proton therapy. *Journal of Radiotherapy in Practice*. 22(e90), 1–5. doi: [10.1017/S1460396923000134](https://doi.org/10.1017/S1460396923000134)

Received: 4 November 2022

Revised: 14 February 2023

Accepted: 20 February 2023

Author for correspondence:

Salahuddin Ahmad, Department of Radiation Oncology, University of Oklahoma Health Sciences Center, Stephenson Cancer Center, 800 NE 10th Street, SCC L 100, Oklahoma City, OK 73104, USA.

E-mail: Salahuddin-ahmad@ouhsc.edu

A Monte Carlo study of the dose enhancement effects of high-z foils in proton therapy

Kristen Duke, Salahuddin Ahmad  and Andy Lau

Department of Radiation Oncology, University of Oklahoma Health Sciences Center, Oklahoma City, OK, USA

Abstract

Background: This investigation quantifies the dose enhancement effect and dose distribution modifications due to the presence of high-z nanospheres in a proton beam.

Methods: Various proton pencil beams of therapeutic energies (60–226 MeV) and spatial distribution of 2.7 mm spot size diameter were simulated onto a water phantom utilising the TOPAS Monte Carlo toolkit version 3.6.1. The simulation modelled either water or nanospheres of high-z materials (gold, silver or platinum) at the location of the Bragg Peak (BP) to compare the differences of the resulting dose distributions.

Results: The introduction of the nanospheres increases the maximum dose, narrows the BP and shifts the BP location upstream compared to the water phantom with no nanospheres.

Conclusions: This work shows that the local dose can be enhanced with the use of high-z nanoparticles in proton therapy, thereby increasing patient safety and decreasing side effects with the same amount of delivered radiation.

Introduction

The purpose of this investigation is to quantify the dose enhancement effects of high-z materials in a proton beam, with extension and verification of previous study.¹ Nanoparticles have been used in nanomedicine to target tumour cells for chemotherapy. Nanoparticles can be engineered with specific shapes, sizes, target ligands and surface properties to bind to cancerous cell receptors, enhance permeability and other pathophysiological effects. These can be combined with therapeutic agents to directly target cancer cells.² These particles have been investigated into use in radiation therapy to act as a radiosensitiser and localise dose to cancerous tissues. Like the use in drug delivery, metal nanoparticles can be used to enhance the likelihood of radiation damage to targeted tumour cells.³

High-z nanoparticles, such as gold, silver and platinum, have additional electrons for incoming radiation to interact with and create secondary electrons. These electrons produce more indirect and direct DNA damage and cause additional dose to be deposited locally. Since nanoparticles can be engineered to target cells and permeate through the cell barrier, electrons can be produced inside cancerous cells as opposed to healthy cells and cause greater damage for the same amount of radiation received. Additionally, noble metal nanoparticles have higher energy of the surface plasmon than the ionisation potential. Plasmons are delocalised electrons that are excited in a material and can release an electron when de-excited. The presence of a higher surface plasmon energy causes a greater amount of electron ejections from noble metals than for non-noble metals with lower surface plasmon energies.⁴

It has been found that the maximum cellular uptake occurs for nanoparticles between 20 and 60 nm, with 50 nm being the 'optimal size'.⁴ The larger the size of the particle, the more interactions occur within the particle itself, resulting in less dose deposited in the medium outside of the nanoparticle.⁴ This study will investigate the dose enhancement effects and the shift in the Bragg Peak (BP) location due to these metallic nanoparticles.

Materials and Methods

A custom simulation was created with Topas 3.6.1, a Monte Carlo toolkit⁴, based on Geant4. The modular physics list used included g4em-standard_opt3, g4h-phy_QGSP_BIC_HP, g4decay, g4ion-binarycascade, g4h-elastic_HP and g4stopping. The applications from these physics lists are shown in Table 1.

A target control phantom of 30 cm × 30 cm × 40 cm of pure water was created. A second custom phantom of pure water was also created with foils of various high-z materials placed inside, as shown in Figure 1. The foils were silver, gold and platinum with widths of the 80–80% BP width in water for the same energy simulated. The phantoms were irradiated with a proton beam with energies of 60, 100, 160 and 226 MeV. The proton beam had a spot size of 2.7 mm, with a flat beam position distribution, an elliptical beam shape and a Gaussian angular distribution. The placement and width of the foils at each energy are shown in Table 2.

© The Author(s), 2023. Published by Cambridge University Press. This is an Open Access article, distributed under the terms of the Creative Commons Attribution licence (<http://creativecommons.org/licenses/by/4.0/>), which permits unrestricted re-use, distribution and reproduction, provided the original article is properly cited.

Table 1. Application of physics lists used for the custom modular physics list, data⁵⁻⁷ are used.

Physics list	Application
g4em-standard_opt3	Medical electromagnetic processes
g4h-phy_QGSP_BIC_HP	Quark gluon string model, uses Geant4 Binary cascade for primary protons and neutrons below ~10 GeV, and a high precision neutron transportation package
g4decay	Decay at rest and in flight
g4ion-binarycascade	Intra-nuclear cascade calculations
g4h-elastic_HP	Geant4 Hadron Elastic Physics with the neutron high precision model
g4stopping	Geant4 Stopping Physics

Table 2. Foil width and placement for various energies.

60 MeV		100 MeV	
Foil width (mm)	Foil location (cm)	Foil width (mm)	Foil location (cm)
0.9	2.94	2.0	7.45
160 MeV		226 MeV	
Foil width (mm)	Foil location (cm)	Foil width (mm)	Foil location (cm)
4.8	17.14	8.0	31.19

The dose enhancement factor (DEF) is defined as follows:

$$\text{DEF} = \frac{\text{Normalized dose from high-}z\text{ phantom}}{\text{Normalized dose from control phantom}} \quad (1)$$

Dose was scored for each simulation in 0.1 mm resolution and 5 million histories were run for each calculation. For each output, the DEF was calculated for each scored point using equation (1) to quantise the increase in dose due to the specific metal foil. The normalised dose was the raw dose divided by the maximum dose for each simulation. The width of the BP was calculated, and the narrowing of the peak for each simulation was then found. Finally, the shift in the BP location was also found.

Planning this experiment was difficult due to limitations in computer power and software. Simulations were initially run on a private Dell PowerEdge T630 with a Linux system. The first theorised setup was a series of 50 nm particles arranged into walls of foils of 50 nm × 30 cm × 30 cm with 50 nm water slices in between each 'foil' for varying densities of metals as shown in Figure 2. For one density, over 2 million individual metal particles were needed.

This simulation would account for the size of a 50 nm particle that is an ideal radiosensitiser taken up into a tumour cell. Different densities of high-*z* foils were calculated to align with densities used in the reference experiment.¹ The radius of each particle was set as 25 nm, and the densities of gold, silver and platinum used were 19.3 kg/m³, 10.49 kg/m³ and 21.45 kg/m³.

The current computer hardware proved to be insufficient to run this simulation. Simulations were then run on the Supercomputing Center for Education and Research's (OSCER) supercomputer

within our university, with a job time limit of 7 days. Unfortunately, the simulation did not complete within the time frame, and a second geometrical setup had to be created to account for the limit in hardware and time.

The second simulation was a condensed version of the first with 50 nm × 30 cm × 30 cm solid foils with interslice water of 50 nm. The number of foils needed per cm was calculated with equation 2 shown below for each referenced density.

$$\text{Foils per centimeter} = \sqrt[3]{\text{solution density} * [\text{particle density} * \text{sphere volume}]^{-1} * [1000^{-2}]} \quad (2)$$

This simulation created over 18,000 metal foils and again failed to run during the allotted time period on OSCER. Our final simulation was found to be one that balanced the run limit of 7 days with the geometry required to properly model the use of nanoparticles on increase in dose deposition. Inter-foil water slices were removed to create a solid foil, as seen in Figure 3, with widths of the foil used in Table 2.

Results

The overall BP shifts, DEFs and BP narrowing for each energy have been shown in Table 3. Shifts in the high-*z* foil BPs are shown in Figure 4 for 226 MeV protons. The DEF for 226 MeV protons is shown in Figures 5. The shifts in the BPs and the DEF for all other energies (Figures 6–15) are included in the Supplemental Materials.

Discussion

Due to the different geometry, simulation codes and the use of a solid foil instead of nanofoils, BP shifts were found to be larger than the reference experiment¹ with 60 and 226 MeV platinum shifts found to be 0.8 mm and 11.1 mm compared to the shifts of 0.43 mm and 5.3 mm in the reference experiment for the nanoparticle density of 6.5 mg/ml. However, longitudinal BP shift follows the pattern of increasing with both proton beam energy and increase in atomic number of the foil.

The narrowing of the 80–80% also followed the reference paper but was again significantly larger due to the use of a solid foil. The greatest narrowing of the 80–80% window was found to be –91.3% for platinum in the 226 MeV beam, compared to –39.38% for the same material and energy in the reference literature at 6.5 mg/ml density. The lowest narrowing percentage was 66% for silver in the 60 MeV beam. The results show that with increasing energy and increasing atomic number, the narrowing of the BP will also increase.

The DEF also followed the same pattern. The greatest DEF was found to be 1.69 for platinum in the 226 MeV beam, and the lowest was found to be 1.41 for silver in the 60 MeV beam. Compared to the literature¹, the DEFs overall were significantly larger than expected. For 226 MeV at 6.5 mg/ml, the reference literature shows a DEF of 1.066 for platinum. The increase could again be attributed to the use of a solid foil with the width of the 80–80% BP as opposed to nanofoils of 6.5 mg/ml density.

While this study focuses on nanofoils due to computational limitations, the next step of modelling nanoparticles has direct clinical impact. As discussed in the introduction, nanoparticles can be bioengineered to directly target and attach to and enter tumour cells and act as a radiosensitiser. When the metallic

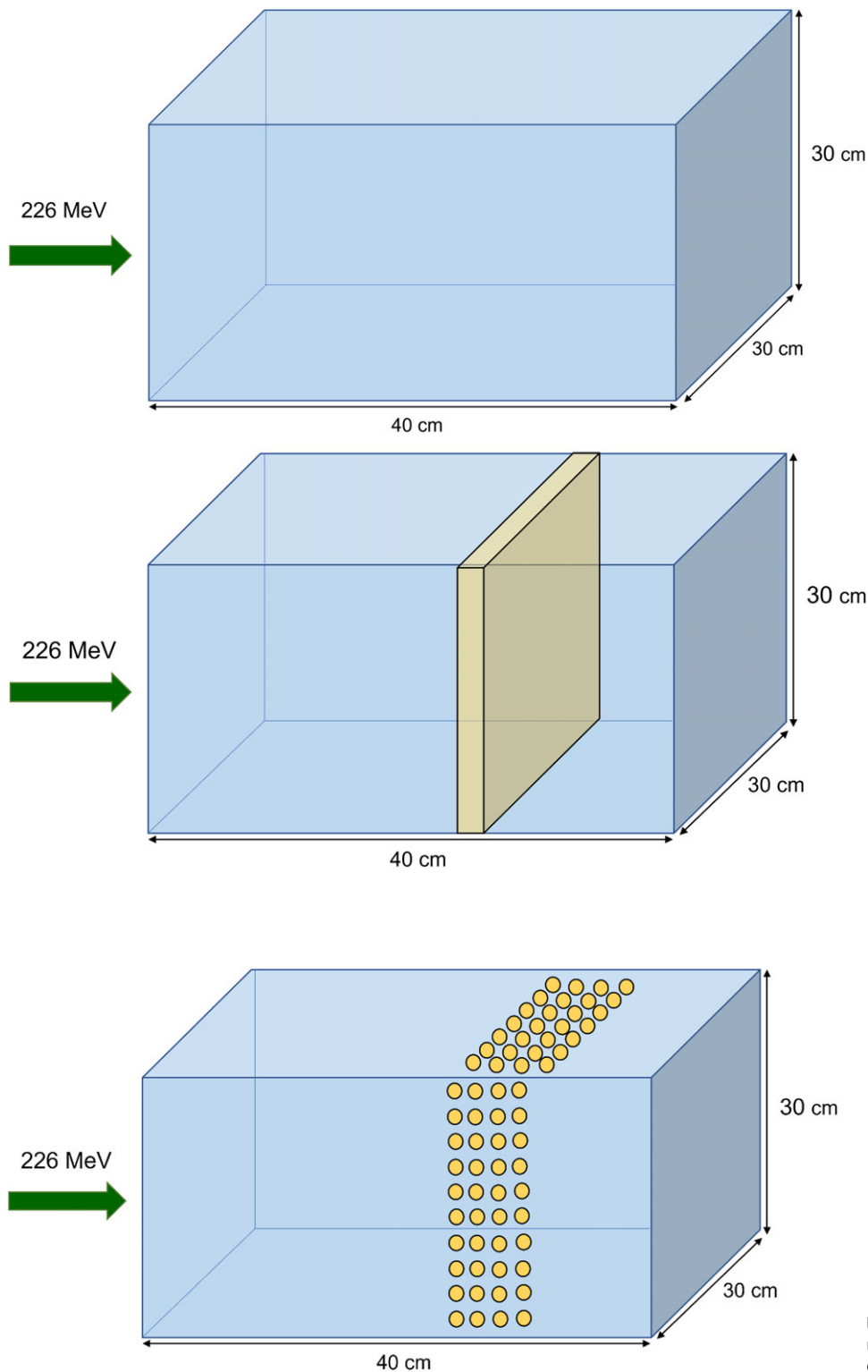


Figure 1. Phantom geometries. (Upper) Empty control water phantom with 226 MeV proton beam. (Lower) Water phantom with high-z metal foil placed in 80–80% Bragg Peak, with a 226 MeV proton beam.

Figure 2. Initial geometry, with 50 nm individual metal particles arranged into walls of 'foils' for a desired high-z density (not to scale).

nanoparticle interacts with radiation, the secondary electrons created travel short distances within the tumour cell itself, causing more damage to the targeted cell and an increase in the DEF as shown in the experiment with nanofoils. With this increase in the DEF, a patient with nanoparticles can receive a greater level of dose to tumour cells, due to the secondary electron creation, with the same level of radiation administered. Additionally, the patient could also instead receive similar tumour doses as

treatments without nanoparticles, but with an overall smaller amount of radiation given to the patient. This would lead to the patient experiencing less side effects and less toxicity to normal tissues, and greater targeted cell killing.

In the future, we plan to submit simulations with the full nanosphere geometry for a more accurate description of the following criteria: dose distribution, the DEF, the location of the BP and the narrowing of the BP, when our computing resources have

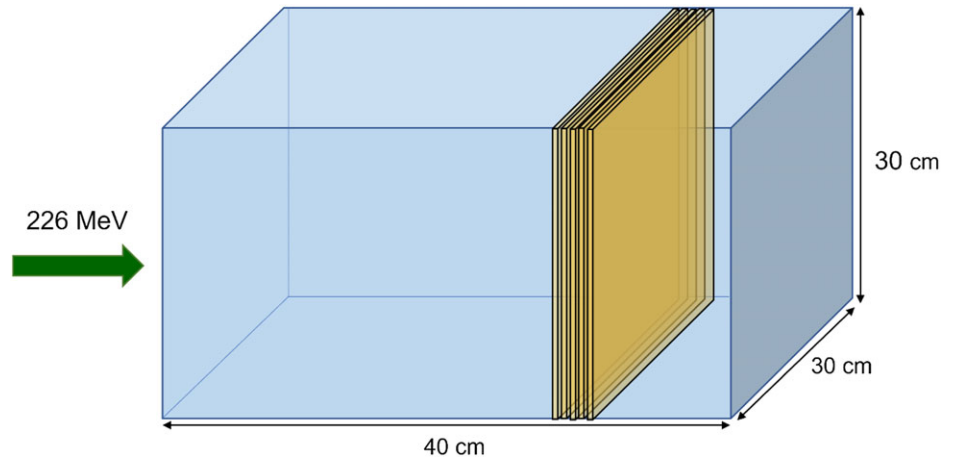


Figure 3. Initial small scale phantom setup showing 50 nm foils with 50 nm water spacing in between.

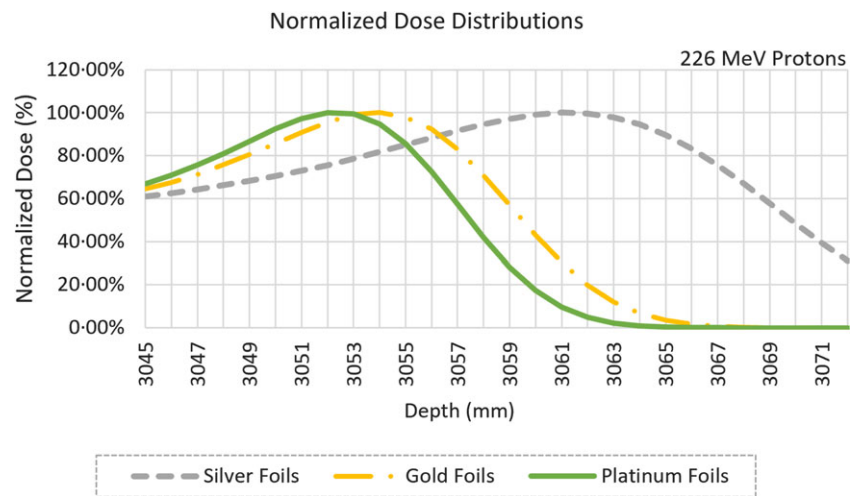


Figure 4. 226 MeV Bragg Peak shifts of silver, gold and platinum foils for depth 30.45–30.72 cm.

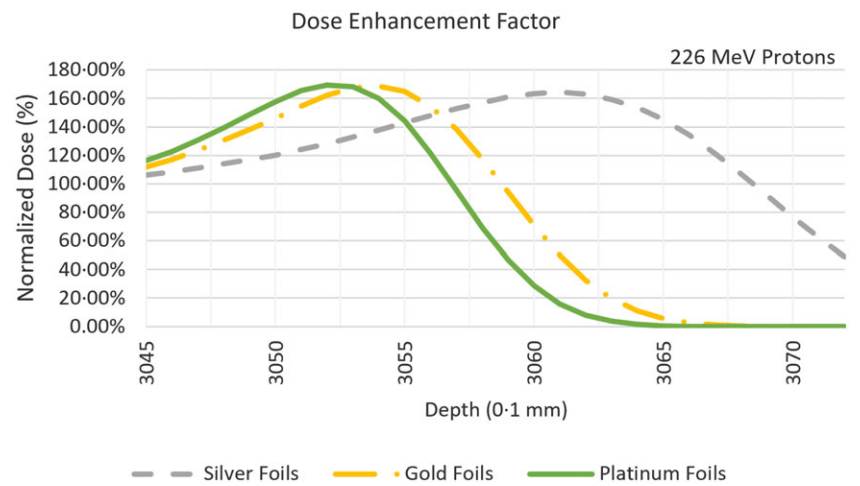


Figure 5. Dose enhancement factor of silver, gold and platinum foils at 226 MeV.

increased. Our current results show the overall trends of the above-mentioned criteria when high-z nano-structures are used in proton therapy simulations.

Although this work focused on the disturbance of the dose distribution from high-z nano-structures, the use of nanospheres in

proton therapy is still a developing area of therapy. There are many questions remaining about the implementation of nanospheres for proton therapy, from diagnostic imaging corrections to image-guidance setup issues as examples. Future work about the implementation is needed for a robust proton therapy treatment.

Table 3. Bragg Peak (BP) shifts upstream, narrowing and dose enhancement factors of 60, 100, 160 and 226 MeV for silver, gold and platinum.

Material	BP (cm)	BP shift (cm)	DEF	80–80% (mm)
60 MeV				
Water	2.98			0.9
Silver	2.91	0.07	1.41	0.3
Gold	2.9	0.08	1.47	0.3
Platinum	2.9	0.08	1.47	0.3
100 MeV				
Water	7.58			2
Silver	7.32	0.26	1.53	0.4
Gold	7.30	0.28	1.57	0.3
Platinum	7.29	0.29	1.59	0.3
160 MeV				
Water	17.44			4.8
Silver	16.8	0.64	1.59	0.8
Gold	16.75	0.69	1.64	0.6
Platinum	16.74	0.70	1.64	0.5
226 MeV				
Water	31.63			8
Silver	30.61	1.02	1.64	1.3
Gold	30.54	1.09	1.69	0.8
Platinum	30.52	1.11	1.69	0.7

Conclusions

Overall, the BP shifts, DEFs and narrowing of the BP of each energy followed the expected trends of the reference work, with greater energies having larger shifts and narrowing of the 80–80% BP

width. Future work on this topic includes different geometrical setups and investigation into the dose enhancement effects of nanospheres and single nanoparticles. With the use of more intense software and computer hardware, our initial geometries could be used to model both nanofoils and nanoparticles aligned into foils with different densities to better compare with the referenced literature. Additionally, a TOPAS toolkit NBio will be used to model the dose enhancement effects of individual nanoparticles on DNA. Biological and chemical processes can be quantised to observe the increase in the number of single and double strand DNA breakage on various types of cells and plasmids due to high-z nanoparticles.

Acknowledgements. None.

Financial Support. None.

Conflict of Interest. None.

References

1. Ahmad R, Royle G, Lourenco A, Schwarz M, Fraechiolla F, Ricketts K. Investigation into the effects of high-Z nano materials in proton therapy. *Phys Med Biol* 2016; 61 (12): 4537–4550.
2. Sun T, Zhang Y, Pang B, Hyun D, Yang M, Xia Y. Engineered nanoparticles for drug delivery in cancer therapy. *Angewandte Chemie (International Ed. in English)* 2014; 53 (46): 12320–12364.
3. Duke K. A Monte Carlo Study of The Dose Enhancement Effect of High-Z Foils in Proton Therapy. M.S. Thesis, The University of Oklahoma Health Sciences Center. 2022.
4. Haume K, Rosa S, Grellet S et al. Gold nanoparticles for cancer radiotherapy: a review. *Cancer Nanotechnol* 2016; 7 (1): 8.
5. CERN accelerating science. Reference Physics Lists; 2022. <https://geant4.web.cern.ch/node/155>
6. Wright D, Incerti S. A short guide to choosing physics list; 2022. http://geant4.in2p3.fr/IMG/pdf_PhysicsLists.pdf
7. TOPAS. Modular physics lists. Modular Physics Lists - TOPAS 3.7 documentation; 2022. <https://topas.readthedocs.io/en/latest/parameters/physics/index.html>